Effect of Mass Transfer on Laminar Jet Breakup:

HARRY C. BURKHOLDER and JOHN C. BERG

Department of Chemical Engineering BF-10
University of Washington, Seattle, Washington 98195

Part I. Liquid Jets in Gases

The instability and breakup of laminar liquid jets in gaseous surroundings is investigated for conditions under which a solute is transferring across the jet interface rendering the system susceptible to Marangoni convection. Linear hydrodynamic stability analysis reveals that solute transfer out of the jet is stabilizing (produces longer jets) while transfer into the jet is destabilizing and promotes breakup. Solute adsorption, including as a limiting case the presence of a spread surfactant monolayer, may strongly counteract the stabilizing or destabilizing effects of mass transfer but has only a negligible effect on jet stability in the absence of interphase mass transfer. Qualitative experimental results for water jets in air with acetone as the transferring solute corroborate both the stabilizing and destabilizing mass transfer effects predicted by the theory.

SCOPE

The problem of the breakup of laminar liquid jets has played a central role in the development of the technique of linear hydrodynamic stability analysis dating back to Rayleigh's pioneering studies (Rayleigh, 1878, 1879). Subsequent refinements of the theory, primarily those of Weber (1931), validated the analytical technique and brought its predictions into substantial agreement with experiment for pure, nonvolatile liquid jets in air. Laminar jet breakup has in the meantime become important in many practical applications including gas absorption or stripping in spray towers, fuel injection, fiber spinning, and others. In many of the above situations, jet breakup is accompanied by mass transfer to or from the jet. While such mass transfer may have a substantial effect on the jet breakup, such as producing longer or shorter jets prior to their disintegration and variations in the ultimate drop size, neither a theoretical analysis nor an experimental study has yet been directed toward elucidating this effect. Its potential importance can be inferred from reports of seemingly anomalous breakup behavior in systems in which it is known that mass transfer is occurring (compare, for example, Prandtl 1952, p. 326) and from speculations in the literature (for example, Sawistowski, 1971) based upon observations of the breakup of liquid films in packed absorption and distillation towers.

The potential influence of mass transfer on the jet breakup derives from the potential in such cases for the development of longitudinal variations in composition along the jet surface prior to breakup. These in turn create corresponding variations in surface tension along the jet which may generate internal flows (Marangoni effect) which can either reinforce or inhibit the growth of the surface corrugations which ultimately lead to breakup of the jet, as first elucidated by Rayleigh. The present investigation (1) examines the mass transfer effect theoretically using linear stability analysis applied to a model of a dilute binary liquid jet to or from which a solute is transferring, and (2) corroborates qualitatively the results of the theory with experiments on the breakup of water jets in air with acetone as the transferring solute.

The problem of determining mass transfer effects on the breakup of liquid jets in liquids, of potential importance in liquid-liquid extraction, is considered in another paper (Burkholder and Berg, 1974).

CONCLUSIONS AND SIGNIFICANCE

The most important predictions of the analysis are: (1) mass transfer of a surface tension lowering solute out of the jet is strongly stabilizing (produces longer jets) and into the jet is strongly destabilizing (produces shorter jets); (2) solute adsorption may strongly counteract either the stabilizing or destabilizing effects of the mass transfer on the jet; (3) solute adsorption, including that of strong surface active agents, has only a very small effect on jet stability in the absence of mass transfer; (4) the wavelength of the most unstable disturbance, hence the ultimate drop size, increases for transfer of a surface tension lowering solute out of the jet (and decreases for transfer into the jet); and (5) the jet may be unstable to asymmetric disturbances under certain conditions during mass trans-

Correspondence concerning this paper should be addressed to J. C. Berg. H. C. Burkholder is with Battelle Northwest, Richland, Washington.

fer (it is always stable with respect to such disturbances for low velocity jets in the absence of mass transfer).

The predicted mass transfer effects on jet stability are qualitatively confirmed by experiments with acetone transferring between a water jet and air. Acetone transfer out caused stabilization, and transfer in caused destabilization. Contrary to the theory, mass transfer did not appear to change significantly the wavelength of the most unstable disturbance, as evidenced by the constancy of the drop size. This discrepancy is attributed to the simplicity of the theoretical model, which does not account for the strong nonlinearity of the radial concentration profile in the jet.

The problem provides a useful illustration of the use of boundary conditions in the study of interfacial hydrodynamics, and of coupled stability phenomena, and its solution may have important implications for industrial operations involving the breakup of liquid jets.

In accord with early observations of the breakup of pure liquid jets (for example, Savart, 1833, Plateau, 1876) and with the postulates of Lord Rayleigh who first analyzed the problem, when a liquid issues from a small circular orifice it is subject to the continual influence of small disturbances whose amplitude grows approximately exponentially with time as the system seeks to minimize its surface area. Depending upon fluid properties and conditions of the experiment, disturbances of a particular wavelength are amplified in preference to all others and appear as regular corrugations on the jet surface, as shown schematically in Figure 1. These ultimately break the jet into drops when their amplitude approximates the jet radius. The growing disturbance is thus represented as the preferentially amplified Fourier component of a general disturbance:

$$\eta = Re\ \{\eta_0\ e^{\beta t + ikz + ih\theta}\} \tag{1}$$

where η is the displacement of the jet surface from its mean position and h is the number of axes of symmetry (either 0, for axisymmetric disturbances, or 1, for asymmetric disturbances). The linear hydrodynamic stability analysis of pure liquid jets requires that the disturbance described by Equation (1) satisfy the linearized Navier-Stokes equations subject to the appropriate boundary conditions, which include, of central importance, the radial force balance showing the pressure drop required to support the curvature of the deformed surface. The analysis then yields the maximum growth constant β^* and the corresponding wave number k^* for the fastest-growing axisymmetric disturbance component. The jet length L and the drop volume V_d are then predicted as

$$L = \frac{U}{\beta^*} \ln \frac{a}{\eta_0} \tag{2}$$

and

$$V_d = \frac{2\pi^2 a^2}{k^*} \tag{3}$$

respectively.

Using his technique, many subsequent investigators generalized Rayleigh's treatment to more realistic situations than that of the inviscid jet in a vacuum treated in Rayleigh's analysis (Rayleigh, 1879).* Notably, Weber (1931) is credited with being first to obtain results for a viscous jet in relative motion (yielding an aerodynamic effect) through an inviscid medium and for having shown that in this case asymmetric disturbances [$h = 1$ in Equation (1)] might be amplified if the jet velocity were sufficiently large. Sterling (1969) and Burkholder (1973) have reviewed the extensive literature on jet breakup, and the former has obtained a general characteristic equation for pure liquid jets in inviscid media which includes the results of most previous investigations as special cases. Weber's predictions of jet length and drop size conform quantitatively to experimental results for low velocity jets (where aerodynamic effects are secondary) and qualitatively for higher velocity jets (Haenlein, 1932).

The effect of mass transfer on jet length and drop size has not yet been considered either theoretically or experimentally, although transfer induced instability at planar interfaces has received much attention following the pioneering studies of Pearson (1958) and Sternling and Scriven (1959). These investigators sought to delineate conditions favorable to the self-amplification of small disturbances into cellular convection or interfacial turbulence

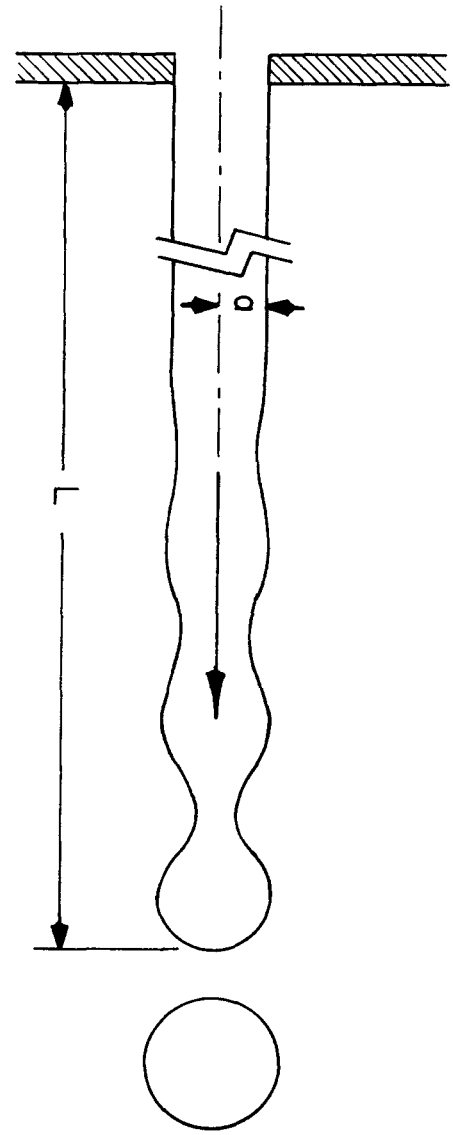

Fig. 1. Schematic diagram of jet breakup.

*Rayleigh also considered the effect of relative motion for a jet free of surface tension (1878), and later, the case in which viscous effects were present but inertial effects neglected (1892).

driven by surface tension variations. Other investigators, for example, Linde et al. (1964), have shown that any inherent asymmetry in the transfer system, such as that which obtains in the vicinity of a curved meniscus (compare Kayser and Berg, 1971) may lead to the development of significant surface tension variation and to convection which is thereby generated and sustained. Such phenomena, known collectively as the Marangoni effect, should be expected to exert an influence upon the Rayleigh mechanism of jet breakup, and the present work is directed toward elucidating it by both analysis and experiment for liquid jets in gases.

THEORETICAL DEVELOPMENT

The model to be analyzed is an infinite, cylindrical column of nonvolatile, incompressible, Newtonian liquid in steady laminar plug flow through an inviscid medium in the absence of external force fields. The plug flow assumption is an approximation, and there are some indications that the state of the initial velocity profile may have a significant effect on the breakup behavior under certain conditions (compare Sterling, 1969; Ling and Reynolds, 1973). The system is isothermal, and a solute is present in small amounts in both phases. The surface is assumed to be in local adsorption equilibrium with both the adjacent bulk phases, and in the undisturbed state, solute concentration varies linearly with radial position within the jet and is uniform in the surroundings. All bulk fluid properties are constant, and surface tension varies linearly with solute concentration at the surface.

A small disturbance, in accord with Rayleigh's postulates, is imposed upon the system producing a deflection of the jet surface and perturbations in the radial and axial velocity components, pressure, and solute concentration. As a consequence, the surface tension and the external phase mass transfer coefficient may vary. In this analysis the variation of all quantities, except the surface deflection, in the azimuthal (θ) direction is neglected.*

In terms of a cylindrical coordinate system moving with the jet, the growth of the perturbations is described by the linearized Navier-Stokes and diffusion equations:

$$\nabla \cdot \underline{u} = 0 \tag{4}$$

$$\nabla \cdot \hat{\underline{u}} = 0 \tag{5}$$

$$\frac{\partial \underline{u}}{\partial t} = -\frac{1}{\rho}\nabla p + \nu \nabla^2 \underline{u} \tag{6}$$

$$\frac{\partial \hat{\underline{u}}}{\partial t} - U\frac{\partial \hat{\underline{u}}}{\partial z} = -\frac{1}{\hat{\rho}}\nabla \hat{p} \tag{7}$$

$$\frac{\partial c}{\partial t} + u_r \frac{\partial c_0}{\partial r} = \mathcal{D}\nabla^2 c \tag{8}$$

where r is the radial coordinate measured from the jet axis, u is the velocity perturbation in the jet (and $\hat{u}$ that in the surroundings) and u_r its radial component, p is the pressure perturbation in the jet (and $\hat{p}$ in the surroundings), c is the solute concentration perturbation in the jet and c_0 the undisturbed concentration, and $\hat{\rho}$ is the density in the surroundings.

Again in accord with Rayleigh, the dependent variables are all given forms consistent with Equation (1), and separation of variables is assumed to apply such that the pre-

*It will be shown later that this simplification leads to a reasonable consideration of asymmetric disturbances.

exponential factor in each case is a function of r only.

The equations are solved subject to linearized boundary conditions which express continuity of velocity, stress, and solute mass flux at the jet surface $r = a$. These take the form:

$$u_r = \frac{\partial \eta}{\partial t} \tag{9a}$$

$$\hat{u}_r = \frac{\partial \eta}{\partial t} - U\frac{\partial \eta}{\partial z} \tag{9b}$$

, surface kinematic condition

$$\mu\left(\frac{\partial u_z}{\partial r} + \frac{\partial u_r}{\partial z}\right) - \left(\frac{\partial \sigma}{\partial c}\right)_0 \frac{\partial c}{\partial z} = 0, \tag{10}$$

continuity of tangential stress,

$$\hat{p} - p + 2\mu\frac{\partial u_r}{\partial r} - \frac{\sigma_0}{a^2}(1 - h^2 - k^2a^2)\eta + \left(\frac{\partial \sigma}{\partial c_0}\right)\frac{c}{a} = 0, \tag{11}$$

continuity of normal stress, and

$$\delta\left[\frac{\partial c}{\partial t} + c_0\left(\frac{u_r}{r} + \frac{\partial u_z}{\partial z}\right)\right] + \mathcal{D}\frac{\partial c}{\partial r} + K_0 c + K(c_0 - c^*) = 0, \tag{12}$$

continuity of solute flux

where δ is the adsorption equilibrium constant with respect to the liquid phase and defined by $\Gamma = \delta c_s$, c_s is the solute concentration in the liquid sublayer, K is the mass transfer coefficient perturbation in the external phase; subscript 0 refers to undisturbed values, subscripts r and z refer to radial and axial components; $\hat{}$ refers to quantities in the surroundings, and c^* is the concentration of solute in the liquid jet that would be in equilibrium with the undisturbed concentration in the surroundings. It should be noted that K and K_0 are actually mass transfer coefficients in the surroundings times the assumed constant solute distribution coefficient between the surroundings and the jet.

Equations (10) and (11) differ from their counterparts for jets without mass transfer by their inclusion of the terms $(\partial\sigma/\partial c)_0\, \partial c/\partial z$, representing the surface shear stress due to surface tension variation caused by axial concentration variation, and $(\partial\sigma/\partial c_0)\, c/a$, the change in capillary pressure due to the dependence of surface tension on concentration. Surface viscosity terms are not included in Equation (10) because they have been shown to be negligible in similar problems (compare Berg and Acrivos, 1965; Palmer and Berg, 1972).

The terms in Equation (12) represent, from left to right, accumulation of solute at the surface, surface convection, diffusive flux to the surface from the interior of the jet, flux of solute from the surroundings, and variation in flux from surroundings due to variation of the mass transfer coefficient. It is anticipated that this latter term is maximum at the disturbance crest and minimum at the valley. Surface diffusion is not included as it is expected to be negligible compared with surface convection.

Simultaneous solution of the equations and boundary conditions and nondimensionalization leads to the following characteristic equation:

$$\bar{\beta}^2\left(\xi\frac{I_0(\xi)}{I_1(\xi)}G_1 + N_{DN}\xi\frac{K_0(\xi)}{K_1(\xi)}\right) + \bar{\beta}\left(-iN_{RE}\xi^2\frac{K_0(\xi)}{K_1(\xi)} + 2\xi^2\left[\frac{2\xi_1^2}{\xi_1^2 - \xi^2}\xi\frac{I_0(\xi)}{I_1(\xi)}\right.\right.$$

(continued on next page)

$$- \frac{2\xi^2}{\xi_1^2 - \xi^2} \xi_1 \frac{I_0(\xi_1)}{I_1(\xi_1)} - 1 \Bigg] G_1 \Bigg) - N_{AE}\, \xi^3 \frac{K_0(\xi)}{K_1(\xi)}$$
$$- N_{SU}\, \xi^2 (1 - h^2 - \xi^2) + N_{MA}\, G_1 G_2 (G_3 G_5 - G_4 G_6)$$
$$+ N_{EL}\, G_1 G_2 (G_3 G_7 - G_4 G_8)$$
$$+ \frac{1}{\overline{\beta}} [N_{SM}\, G_1 G_2 (G_3 - G_4)] = 0 \quad (13)$$

where

$$G_1 = \frac{\overline{\beta}}{\overline{\beta} + N_{MA}\, G_2 (G_5 - G_6) + N_{EL}\, G_2 (G_7 - G_8)}$$

$$G_2 = \frac{\xi^2 \dfrac{I_0(\xi_2)}{\xi_2 I_1(\xi_2)}}{1 + \dfrac{I_0(\xi_2)}{\xi_2 I_1(\xi_2)} (N_{SH} + \overline{\beta}\, N_{SS})}$$

$$G_3 = (\xi_1^2 + \xi^2)\xi \frac{I_0(\xi)}{I_1(\xi)}$$

$$G_4 = (\xi_1^2 - \xi^2) + 2\xi^2 \xi_1 \frac{I_0(\xi_1)}{I_1(\xi_1)}$$

$$G_5 = \frac{\int^a s I_0(ms) I_1(ls)\, ds}{a^2 I_0(\xi_2)\, I_1(\xi_1)}$$

$$G_6 = \frac{\int^a s I_0(ms) I_1(ks)\, ds}{a^2 I_0(\xi_2)\, I_1(\xi)}$$

$$G_7 = \xi_1 \frac{I_0(\xi_1)}{I_1(\xi_1)} - 1$$

$$G_8 = \xi \frac{I_0(\xi)}{I_1(\xi)} - 1$$

$$\xi_1 = (\xi^2 + \overline{\beta})^{1/2}$$

and

$$\xi_2 = (\xi^2 + \overline{\beta}\, N_{SC})^{1/2}$$

Equation (13) relates the dimensionless growth constant $\overline{\beta} = \beta \rho a^2/\mu$ to the dimensionless wave number $\xi = ka$ for given sets of values of the ten dimensionless groups describing the properties of the system and defined in Table 1. It contains the results of all previous theoretical analyses of the stability of nonrotating liquid jets in gases in the absence of external force fields as limiting cases. For example, setting N_{MA}, N_{EL}, N_{SM}, N_{SH}, and $N_{SS} = 0$ corresponds to the case of a pure liquid jet and reduces Equation (13) to the characteristic equation of Sterling (1969). On the other hand, setting $h = 0$ (for the case of axisymmetric disturbances only) and N_{RE}, N_{AE}, N_{MA}, N_{SM}, N_{DN}, and $N_{SH} = 0$ corresponds to the case of a liquid jet in a vacuum on whose surface is spread an insoluble, nonvolatile surfactant. Under these conditions, after a small amount of algebra, Equation (13) reduces to the results of Anshus (1973), who studied the effect of insoluble surfactants on jet stability.

In computations based on Equation (13), the imaginary term which describes the relative motion of the surface disturbance to the steady jet velocity in the absence of mass transfer, is neglected. The magnitude of this term is directly proportional to the density of the surroundings and inversely proportional to the viscosity of the jet. Consequently, Sterling (1969) has shown that this imaginary term is always small for jet velocities of practical importance and that the inclusion of it produces a maximum

Table 1. Dimensionless Groups in Equation (13)

$N_{RE} = \dfrac{2a\hat{U}\hat{\rho}}{\mu}$:	Reynolds number
$N_{SU} = \dfrac{\sigma_0 \rho a}{\mu^2}$:	Suratman number
$N_{AE} = \dfrac{\hat{\rho}\rho U^2 a^2}{\mu^2}$:	Aerodynamic number
$N_{MA} = \dfrac{\left(\dfrac{\partial\sigma}{\partial c}\right)_0 \left(\dfrac{\partial c_0}{\partial r}\right) a^2}{\mu \mathcal{D}}$:	Marangoni number
$N_{EL} = \dfrac{\left(\dfrac{\partial\sigma}{\partial c}\right)^2 (\overline{c_0})_a}{RT\mu\mathcal{D}}$:	Surface elasticity number
$N_{SS} = \dfrac{-\left(\dfrac{\partial\sigma}{\partial c}\right)_0 \mu}{aRT\rho\mathcal{D}}$:	Surface Schmidt number
$N_{SM} = \dfrac{\left(\dfrac{\partial\sigma}{\partial c}\right)_0 (c_0 - c^\circ)_a K_c \rho a^3}{\mu^2 \mathcal{D}}$:	Surface disturbance Marangoni number
$N_{DN} = \dfrac{\hat{\rho}}{\rho}$:	Density ratio
$N_{SC} = \dfrac{\mu}{\rho\mathcal{D}}$:	Schmidt number
$N_{SH} = \dfrac{K_0 a}{\mathcal{D}}$:	Sherwood number

error of less than 0.2% in the calculated values for the growth constant and dimensionless wave number of the most unstable disturbance for the case of a liquid jet in relative motion through gaseous surroundings. No additional imaginary terms appear in this more general analysis so that Sterling's conclusion should remain valid here as well. Equation (13) clearly shows that there is coupling of Marangoni effects (as characterized by N_{MA} and N_{EL}) with aerodynamic and capillary instability (as characterized by N_{AE} and N_{SU}, respectively). After further rearrangement it is solved numerically for a number of sets of values for the dimensionless groups, and a modified Fibonacci search is performed for the maximum $\overline{\beta}$ for both the axisymmetric and asymmetric disturbance modes using relaxation and underrelaxation convergence techniques on the largest positive real root at each search point. At the maximum $\overline{\beta}$, the real and imaginary parts of the complex root were calculated if complex roots were present. In all of the calculations with axisymmetric disturbances the real part of the complex root was always negative. This suggests, but does not prove, that the principle of exchange of stabilities is valid for axisymmetric disturbances over the range of practical values of the physical properties and experimental parameters. For asymmetric disturbances the real part of the complex root was sometimes positive but was always at least an order of magnitude smaller than the largest real root. This suggests, but does not prove, that the stationary regime is always dominant for asymmetric disturbances as well over the range of practical values of

the physical properties and experimental parameters. Levich (1962, p. 632) has already shown that the principle of exchange of stabilities is valid for both axisymmetric and asymmetric disturbances for Weber's problem, and the presence of mass transfer does not seem to favor the occurrence of the oscillatory regime.

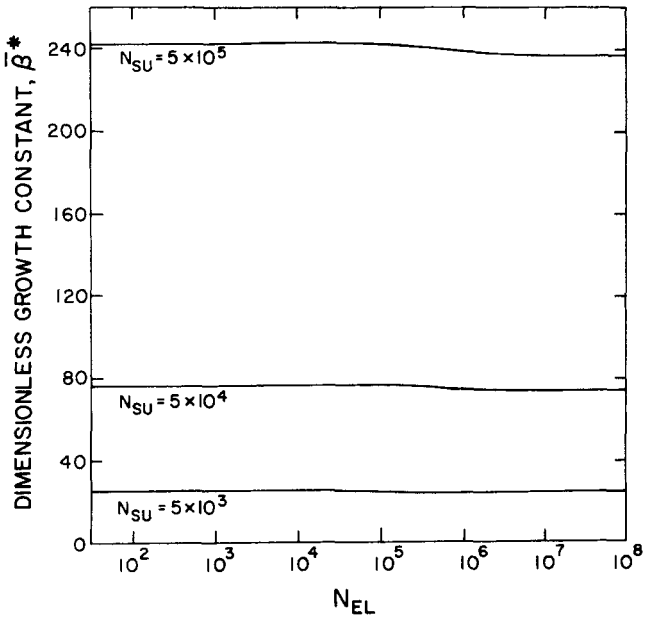

Fig. 2. Dimensionless growth constant vs. elasticity number showing the effect of solute adsorption or the presence of surfactants on jet stability in the absence of mass transfer. Other dimensionless groups have values: $N_{AE} = 10^3$, $N_{MA} = 0$, $N_{SS} = 0.4$, $N_{SM} = 0$, $N_{DN} = 10^{-3}$, $N_{SC} = 10^3$, and $N_{SH} = 10^4$.

THEORETICAL RESULTS AND DISCUSSION

Figure 2 shows the effect of surface adsorption (as characterized by N_{EL}) on the dimensionless growth constant of the most unstable axisymmetric disturbance for various values of N_{SU}, which characterizes the surface tension level. It presents results for the surface adsorption of a volatile soluble surfactant at small rates of mass transfer ($N_{SH} = 10^4$). Results for a nonvolatile, insoluble surfactant ($N_{SH} = 0$) are the same except that the small stabilization occurs at several orders of magnitude smaller values of N_{EL}. As shown, surface adsorption is only weakly stabilizing in the absence of mass transfer (regardless of the value of N_{SU}) even for large surface concentrations of surfactant. The smallness of the stabilization effect is in agreement with the calculations of Anshus (1973) and the speculations of Levich (1962, p. 652) and derives from the smallness of the extent of surface movement (dilation and contraction) required for jet breakup by the Rayleigh mechanism. In contrast, interfacial turbulence can be strongly inhibited by solute adsorption, particularly if the relative adsorption is great. This is because it consists of surface renewal sustained by surface tension gradients which tend to be nullified by the surface redistribution of solute brought about by the surface renewal itself. No such surface tension gradients or surface flows are required in the Rayleigh mechanism of jet breakup.

Figures 3, 4, and 5 show the effect of mass transfer, hence the Marangoni effect as characterized by N_{MA}, on jet stability for various values of N_{SU}, N_{AE}, and N_{EL}, respectively. Again the ordinate in these graphs is the dimensionless growth constant for the preferentially amplified axisymmetric disturbance, and therefore an increase in its magnitude corresponds to a less stable, that is, shorter, jet. The results show that the transfer of a surface tension lowering solute out of the jet may be strongly stabilizing, while transfer into the jet may be strongly de-

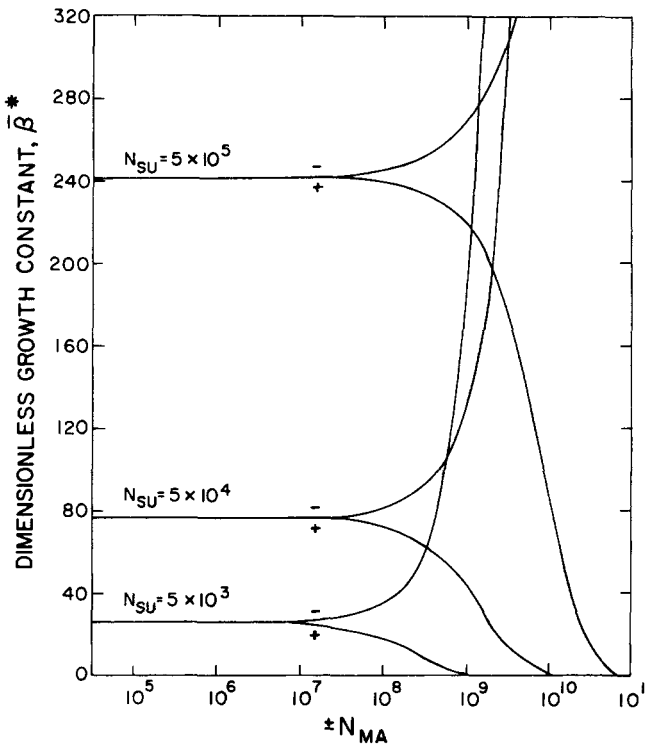

Fig. 3. Dimensionless growth constant vs. Marangoni number. + and − denote the sign of the Marangoni number corresponding to each branch of the curves for various values of N_{SU}. Curves show the effect of mass transfer on jet stability. Other dimensionless groups have values: $N_{AE} = 10^3$, $N_{EL} = 0$, $N_{SS} = 0.4$, $N_{SM} = 0$, $N_{DN} = 10^{-3}$, $N_{SC} = 10^3$, and $N_{SH} = 10^4$.

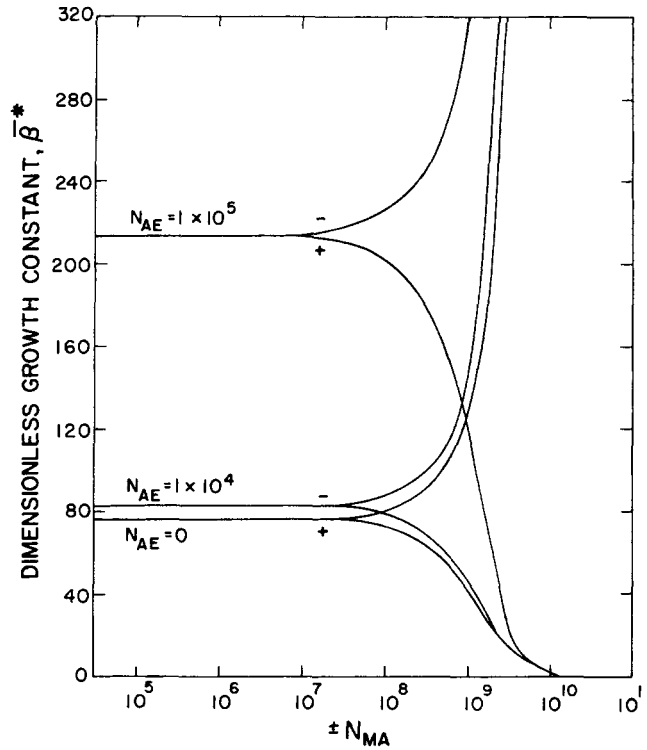

Fig. 4. Dimensionless growth constant vs. Marangoni number (+ and − denote sign of N_{MA}) showing the effect of mass transfer on jet stability for various values of N_{AE}. Other dimensionless groups have values: $N_{SU} = 5 \times 10^4$, $N_{EL} = 0$, $N_{SS} = 0.4$, $N_{SM} = 0$, $N_{DN} = 10^{-3}$, $N_{SC} = 10^3$, and $N_{SH} = 10^4$.

stabilizing. These results may be explained on qualitative physical grounds with reference to Figure 6. Figure 6a shows an undisturbed section of the jet with lines representing constant solute concentration sketched in. The axisymmetric surface deformation of the jet then creates new surface at the crests of the corrugations and reduces surface area at their troughs producing the shift in the lines of constant concentration shown in Figure 6b. The surface of the jet thus becomes relatively richer in solute at the crests than at the troughs for the case of solute transfer out of the jet and thereby reduces the surface tension at the crests relative to that in the troughs (for the usual situation, in which the solute lowers the surface tension). The resulting surface tension gradient then generates a surface flow directed away from the disturbance crests, as shown in Figure 6c, and thereby tends to oppose the necking down process which ultimately causes the jet to disintegrate. One can similarly rationalize the destabilizing effect of the transfer of a surface tension lowering solute into the jet. Both effects would be reversed for a surface tension increasing solute.

The calculations show that the stabilizing or destabilizing effects of mass transfer may be characterized by the Marangoni number and that they start to become significant over a wide range of conditions when the latter parameter reaches values of approximately 10^8. That such values correspond to those that might readily be encountered in practice is demonstrated by numerical examples such as those pertaining to the experiments with acetone transfer between water jets and air described later.

Figure 3 can be used to compare the predicted behavior of a system in the presence and absence of a transferring solute. If the solute lowers the surface tension, its presence will lower the Suratman number, and the jet will become more stable even in the absence of mass transfer, (corresponding to low N_{MA}). For example, for a 2-mm diameter pure water jet in air at room temperature, $N_{SU} \sim 7 \times 10^4$, yielding a dimensionless growth constant, $\bar{\beta}^* \sim 90$. If the presence of the solute reduced the jet surface tension by 10 dynes/cm, $N_{SU} \sim 6 \times 10^4$ and the corresponding $\bar{\beta}^*$

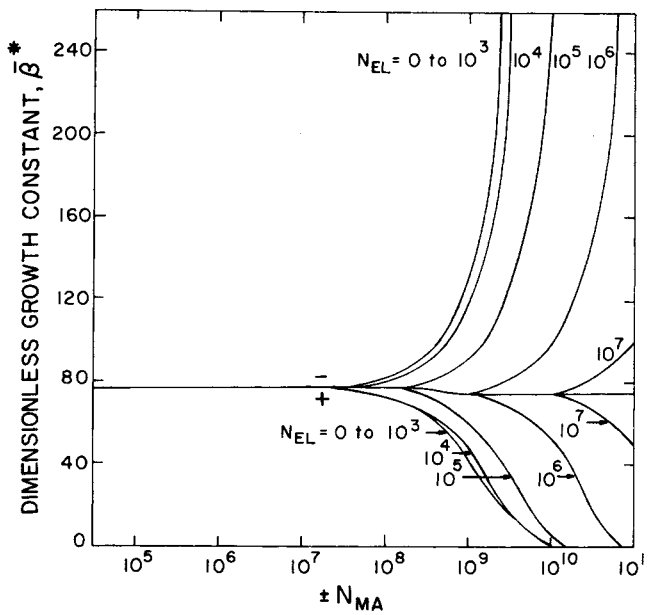

Fig. 5. Dimensionless growth constant vs. Marangoni number (+ and − denote sign of N_{MA}) for various values of the elasticity number showing the effect of mass transfer on jet stability in the presence of solute adsorption or the presence of surface active agents. Other dimensionless groups have values: $N_{SU} = 5 \times 10^4$, $N_{AE} = 10^3$, $N_{SS} = 0.4$, $N_{SM} = 0$, $N_{DN} = 10^{-3}$, $N_{SC} = 10^3$, and $N_{SH} = 10^4$.

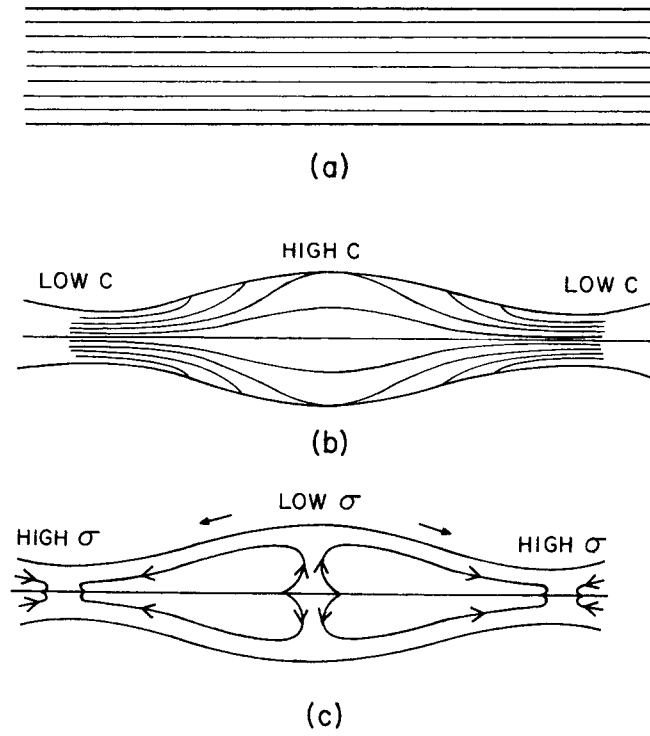

Fig. 6. Schematic diagram showing the influence of the Marangoni effect on jet stability. (a) Undeformed jet with lines indicating constant solute concentration. (b) Deformed jet showing distortion of constant solute concentration lines, (c) Internal flows set up by surface tension variations for the case of a surface tension lowering solute transferring out of the jet.

$\sim$ 80, so that the predicted jet length, which is proportional to $1/\bar{\beta}^*$, would increase by approximately 12%. On the other hand, if the solute were transferring out of the jet such that the Marangoni number were approximately 10^8 (corresponding to a moderate rate of mass transfer), the predicted $\bar{\beta}^*$ becomes approximately 65, corresponding to a predicted increase in the jet length of approximately 38%. Higher rates of mass transfer would yield even greater predicted increases in jet length. Conversely, if mass transfer were directed into the jet, giving negative values of N_{MA}, the predicted $\bar{\beta}^*$ increase due to the Marangoni effect could easily offset the decrease due to surface tension reduction and thereby predict a decrease in jet length.

Figure 4 shows that the predicted mass transfer effects remain intact as the jet velocity increases to the point that aerodynamic effects play a significant role in the jet breakup.

Figure 5 shows the effect of solute adsorption, as characterized by the elasticity number N_{EL}, on jet stability in the presence of mass transfer. As seen, large effective elasticity of the adsorption layer (sometimes termed the *Gibbs layer*) strongly suppresses the Marangoni effect due to mass transfer by shifting the branching of the stability curves due to mass transfer to higher and perhaps unachievable ranges of Marangoni number. In order for adsorption to have an effect at all, the theory shows that the elasticity number must exceed about 1000, and this precludes the likelihood that adsorption of the transferring solute itself will have a significant influence. On the other hand, the presence of nontransferring surfactants may completely suppress either the stabilization or destabilization of the jet due to the presence of a transferring solute. For example, if the water jet described above contained *n*-octanol at a concentration of 10^{-3}M, the corresponding value of

N_{EL} would be approximately 2×10^5, and any stabilizing or destabilizing effects due to the transfer of another solute would not occur until Marangoni numbers at least an order of magnitude larger than required in the absence of surfactant were attained.

Other results obtained for the case of axisymmetric disturbances but not shown in the figures are (1) that any physically reasonable disturbance in mass transfer coefficient in the gas phase, as represented by N_{SM} produces only negligible effects on the predicted $\bar{\beta}^*$, and (2) that stability results depend only very weakly on N_{SS}, and (3) that the effect of increasing N_{SC} or N_{SH} an order of magnitude, other factors remaining constant, is to shift the branch points of the stability curves in Figure 5 to higher Marangoni numbers by factors of approximately seven and ten, respectively.

Figure 7 shows the effect of mass transfer on the dimensionless wave number ξ^* and hence on predicted drop size. The results show that ξ^* becomes large for large negative N_{MA} (that is, transfer of a surface tension lowering solute into the jet) and small for large positive N_{MA} (that is, transfer of a surface tension lowering solute out of the jet). Thus increasing $\bar{\beta}^*$ (decreasing jet length) is always accompanied by increasing ξ^* (decreasing drop volume), and vice versa. As N_{EL} increases, the effect of mass transfer on predicted ξ^* is suppressed as is the effect of mass transfer on $\bar{\beta}^*$.

The effect of mass transfer, for the case of transfer out of the jet, on the growth constant for the asymmetric disturbance mode is shown in Figure 8. For comparison, the curves for the axisymmetric disturbance mode are also sketched in. As the mass transfer rate increases, the asymmetric mode is destabilized while the axisymmetric mode is stabilized. At some transfer rate, which is a strong function of N_{EL}, the $\bar{\beta}^*$ for the asymmetric mode becomes larger than the $\bar{\beta}^*$ for the axisymmetric mode so that the theory predicts that an asymmetric jet deformation might be observed visually, presumably as sinuousity in the jet, before the jet is broken up. Even though the most unstable asymmetric disturbance is growing faster than the most unstable axisymmetric disturbance for high rates of mass transfer, axisymmetric disturbances, of course, continue to control the jet length since the jet must ultimately pinch off into drops. The growing asymmetric disturbances would be difficult to observe, however, because their wave lengths

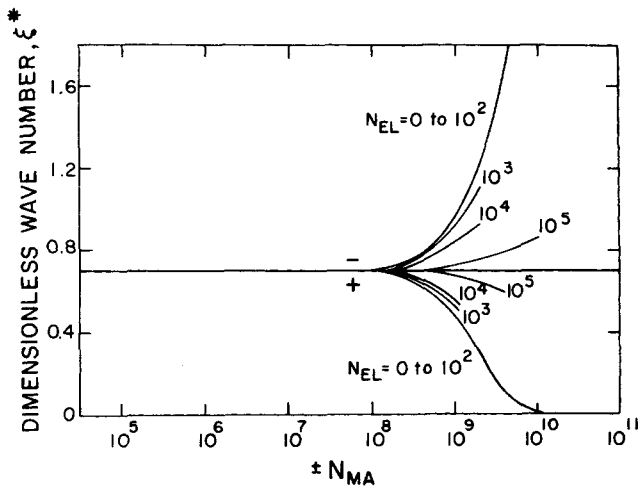

Fig. 7. Dimensionless wavenumber vs. Marangoni number (+ and − denote sign of N_{MA}) for various values of the elasticity number showing the effect of mass transfer on the predicted drop size. Other dimensionless groups have values: $N_{SU} = 5 \times 10^4$, $N_{AE} = 10^3$, $N_{SS} = 0.4$, $N_{SM} = 0$, $N_{DN} = 10^{-3}$, $N_{SC} = 10^3$, and $N_{SH} = 10^4$.

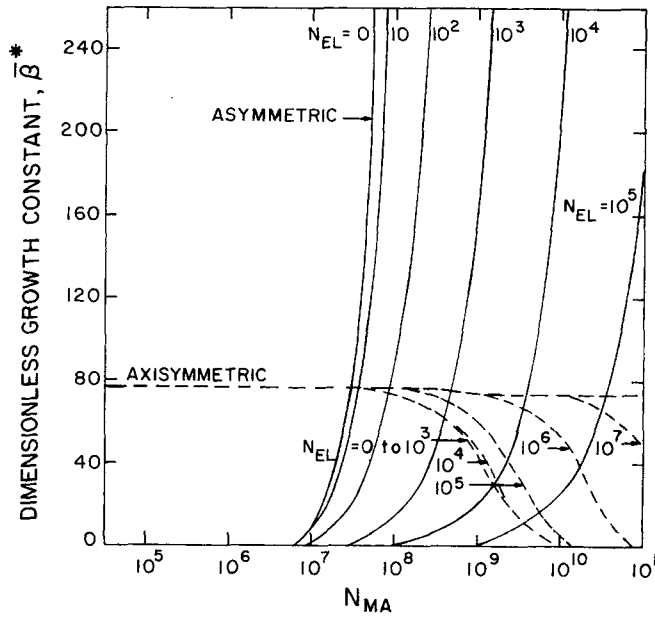

Fig. 8. Dimensionless growth constants for both asymmetric and axisymmetric disturbances vs. Marangoni number for various values of the elasticity number. Other dimensionless groups have values: $N_{SU} = 5 \times 10^4$, $N_{AE} = 10^3$, $N_{SS} = 0.4$, $N_{SM} = 0$, $N_{DN} = 10^{-3}$, $N_{SC} = 10^3$, and $N_{SH} = 10^4$.

are very much smaller than the radius of the jet. It has been suggested (compare Burkholder, 1973) that the jet might be expected to burst into many very fine droplets if the dimensionless growth constant for the asymmetric modes was much greater than that for the axisymmetric mode and the dimensionless wave number was very large. Such bursting was observed by Sterling (and presumably others) for very high velocity jets without mass transfer.

The large dimensionless wave numbers for the asymmetric mode justify a posteriori the assumption that azimuthal gradients in properties other than η are unimportant. Most, if not all, solutions containing volatile, soluble adsorbing solutes have N_{EL} values smaller than 4,000. In this case, the dimensionless wave number of the most unstable asymmetric disturbance is always greater than 10. From the results of Alterman (1961) the assumption is valid if the following equalities are approximately correct:

$$\frac{K_0'(\xi)}{K_0(\xi)} \simeq \frac{K_1'(\xi)}{K_1(\xi)} \quad \text{and} \quad \frac{I_0'(\xi)}{I_0(\xi)} \simeq \frac{I_1'(\xi)}{I_1(\xi)}$$

Calculations for $\xi = 10$ show that these equalities are correct to within approximately 0.5%. Further calculations show that the approximation is even better for larger ξ values.

EXPERIMENT

Experiments were undertaken to test the predicted mass transfer effects on jet breakup. Water jets were formed in air with acetone as the transferring solute; in particular, water-acetone jets with acetone concentrations of 0, 10, 20, 60, 80, and 100 wt. % were contacted with pure air, and pure water jets were contacted with air-acetone mixtures with acetone concentrations of 0.2, 0.4, 1.2, 3.1, 3.3, 7.8, and 8.4 mole %. The apparatus used is shown schematically in Figure 9. Jets were formed by a sharp-edged, 0.168-cm diameter orifice and issued into a breakup chamber 29 × 29 × 4 in. constructed of plywood edges and ¼ in. LOF Paralleleplate® glass windows. The drops from the jet breakup were collected in a metal trough (lined with foam rubber) at the bottom of the chamber and removed through a drain.

Liquid for the jet flowed from a constant head reservoir such

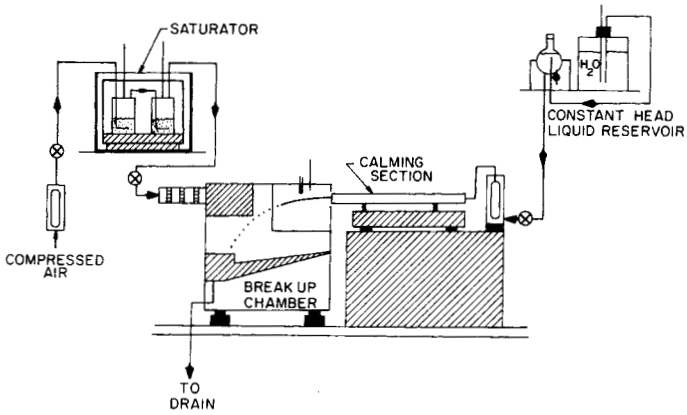

Fig. 9. Schematic diagram of jet breakup—mass transfer apparatus.

that the jet velocity was 136 cm/s in all experiments. Before reaching the orifice, it passed through a flow meter and a 2.5-ft. long calming section consisting of a 1-in. diam. Schedule 40 steel pipe surrounded by 1-in. thick fiberglass insulation and containing 200 and 40 mesh screens and 3 in. of aluminum honeycomb. The calming section rested on a vibration-free table and was connected to a flow meter at the upstream end by a short section of polyethylene tubing which helped to isolate the calming section from vibrations induced by the flow meter. The entire liquid delivery system was not connected rigidly to the breakup chamber; there was a 7/16-in. annular gap between the orifice plate and the chamber wall.

Particular care was taken in construction of the orifice, which was formed at the center of a 2⅛-in. diam. × ⅛-in. thick stainless steel plate. The hole was bevelled back on the downstream side at an angle of 45° to within a fraction of a millimeter of the upstream surface. It was then deburred and polished using jewelers' broaches until it contained no imperfections visible at 30X magnification.

Air, presaturated with water vapor and containing measured concentrations of acetone, entered the breakup chamber opposite the orifice plate after passing through a flow meter and a muffler system. It exited through the annular space surrounding the orifice plate. The muffler contained alternate layers of ½ in. thick foam rubber and aluminum honeycomb and reduced vibrations due to the vapor delivery system. The air flow rate was set at 1.5 liter/s in all experiments.

The disintegrating jets were photographed on 35 mm film using a General Radio Company Type 1531-A Strobotac electronic stroboscope with a 7 microsec flash duration. 18 photographs were taken for each set of experimental conditions, and the jet length determined for each case using a Vanguard Motion Analyzer.

All experiments were performed with Reagent grade acetone and singly distilled water, and while particular attention was given to cleanliness, no special precautions were taken to eliminate surface contaminants. In a typical experiment the air and water flow rates were set and the system permitted to reach steady state, after which a 50-cm³ gas sample was taken from the chamber and the jet photographs taken. The acetone concentration in the chamber atmosphere was determined by analyzing the gas sample by GLC.

EXPERIMENTAL RESULTS AND COMPARISON WITH THEORY

A summary of the experimental results for jet length, together with growth constants computed from them, and Marangoni numbers is contained in Table 2. Runs 1 and 7 are for pure water and pure acetone jets, respectively, while Runs 2 through 6 describe mass transfer out of the jet, and Runs 8 through 14 describe transfer into the jet. It is apparent that the jet lengths for transfer out of the jet are greater than those for transfer into the jet, but because other quantities (surface tension, viscosity, and density) vary simultaneously with the mass transfer rate and direction, the significance of the experimental data and their correspondence with the theory cannot be determined without a more detailed analysis.

First, the computation of $\bar{\beta}^\circ = \beta^\circ \rho a^2/\mu$ from measured jet lengths is based on Equation (2) and requires a value for η_0, the initial disturbance level. This was determined using the theoretically predicted value for $\bar{\beta}^\circ$ for a pure water jet together with the measured jet length for the pure water case, Run 1. η_0 was then assumed to be the same for all subsequent runs.

The severest assumption of the theoretical model, and affecting primarily the determination of the Marangoni number, is that the undisturbed radial concentration gradient ($\partial c_0/\partial r$) is linear and constant along the jet. This in effect assumes a steady line source (or sink) of mass along the jet axis. The experimental situation, on the other hand, is best described in terms of penetration mass transfer into (or out of) a cylinder of initial solute concentration c_i from (or to) an infinite medium of concentration c_∞. Because the jet lifetimes for the experiments ($t = L/U$) are small (~0.15 s), the boundary layer thickness ($\delta_m \sim \sqrt{Dt}$) is small (0.0012 cm) relative to the jet radius (0.076 cm), and the concentration profile is strongly nonlinear. In fact, the jet itself may be considered an infinite medium. Thus only a qualitative comparison between theory and experi-

TABLE 2. SUMMARY OF DATA FOR THE ACETONE-WATER AIR EXPERIMENTS AND THE EXPERIMENTAL $\bar{\beta}^\circ$ VALUES AND N_{MA} RANGES

Run no.	Acetone concentration in water, wt. %	Acetone concentration in air, mole %	Mean jet length (cm) with confidence limit at 95% level	$\bar{\beta}^\circ$	N_{MA} range
1	0	0	17.8 ± 0.4	86.5	
2	10	0.3	20.1 ± 0.4	80.1	6.1×10^7-2.6×10^9
3	20	0.8	21.1 ± 0.5	80.3	7.4×10^7-3.0×10^9
4	60	0.9	25.8 ± 0.6	85.5	1.9×10^8-8.2×10^9
5	80	0.8	24.7 ± 1.5	108	2.5×10^8-1.0×10^{10}
6	90	—	23.9 ± 1.1	126	2.7×10^8-1.2×10^{10}
7	100	0.7	22.0 ± 1.2	156	—
8	0	0.2	17.0 ± 0.4	90.5	-3.1×10^6—1.2×10^8
9	0	0.4	17.9 ± 0.2	86.0	-4.7×10^6—1.8×10^8
10	0	1.2	19.0 ± 0.2	81.0	-1.1×10^7—4.3×10^8
11	0	3.1	18.9 ± 0.2	81.4	-1.9×10^7—7.6×10^8
12	0	3.3	18.5 ± 0.5	83.1	-1.9×10^7—7.6×10^8
13	0	7.8	20.8 ± 0.5	74.0	-2.8×10^7—1.1×10^9
14	0	8.4	20.5 ± 0.8	75.1	-3.1×10^7—1.2×10^9

ment can be made.

The solution for the surface solute concentration $(c_0)_a$ is thus

$$\frac{(c_0)_a - c^*}{c_i - c^*} = \exp\left[\frac{k_0^2 t}{\mathcal{D}}\right] \operatorname{erfc}\left[k_0\sqrt{\frac{t}{\mathcal{D}}}\right] \quad (14)$$

where k_0, the gas phase mass transfer coefficient, is estimated at 4.5 cm/s. The surface concentration reaches a quasi steady value at a very short time relative to the jet surface age at the point of breakup, and an arbitrary value of $t = 0.075$ s is used to compute it from Equation (14). Surface tension data for the acetone-water system (CRC Handbook, 1962) are then used to compute the surface tension and its concentration coefficient.

Computation of effective Marangoni numbers for the experiments is necessarily somewhat arbitrary because its definition in the theory is based on the assumption of a linear undisturbed concentration profile. However, reasonable upper and lower bounds for the effective concentration gradient, and hence N_{MA}, may be obtained as follows. The maximum value of $(\partial c_0/\partial r)_a$ would correspond to the slope of the unsteady profile at the jet surface, that is, $(\partial c_0/\partial r)_a = -\frac{K_0}{\mathcal{D}}(c_0 - c^*)_a$, while the minimum would correspond to $(\partial c_0/\partial r)_a = [(c_0)_a - c_i]/a$. Using both values leads to the N_{MA} range shown in Table 2. CRC Handbook values were used for the remaining properties required in the computation of the various dimensionless groups describing the system.

The theoretical $\bar{\beta}^*$ vs. N_{MA} curves and the $\bar{\beta}^*$ lines for the experiments with mass transfer out of the jet (Runs 2 through 6) are presented in Figure 10. The left end of each experimental β^* line corresponds to the minimum Marangoni number value while the right end of the line corresponds to its maximum. It is seen that the experimentally observed $\bar{\beta}^*$ for each experiment is much smaller than the $\bar{\beta}^*$ expected for that experiment if Marangoni effects had not been present. Thus, mass transfer out of the jet is strongly stabilizing, in qualitative agreement with the theory.

The results for transfer into the jet are shown in Figure 11. The experimentally observed $\bar{\beta}^*$ for each experiment is seen to be slightly larger than the $\bar{\beta}^*$ expected for that experiment if Marangoni effects had not been present so that mass transfer into the jet is destabilizing, again in qualitative agreement with theory. Limitations of the experimental equipment prevented the attainment of larger mass transfer rates into the jet and hence larger destabilizations.

In comparing experimental results with theory, it should be noted, in addition to the theory's physically unrealistic linear concentration profile, it also deals only with dilute solutions whereas some of those encountered in the experiments were quite concentrated. In addition, the presence of possible surface contamination in the experiments might have reduced somewhat the Marangoni effect for transfer in both directions.

Finally, and as a consequence of the theory's linear profile assumption, the predicted mass transfer effect on drop size was not observed. In fact, the observed dimensionless wave number in the experiments was almost constant at a value of 0.7, in almost exact agreement with the value predicted by Rayleigh's initial analysis. Because the penetration depth is only about 2% of the jet radius, the roll cells shown in Figure 6 are probably confined to a very thin region near the jet surface. Thus in the experiments the Marangoni instability apparently affects the growth constant of the most unstable disturbance without greatly affecting its dimensionless wave number. However, in the theoretical model the roll cells involve the entire jet and hence more strongly influence the most unstable wave number. The above result suggests that mass transfer can be used to promote or retard jet breakup without changing the size of the resulting drops in situations where the mass penetration depth is only a small fraction of the jet radius.

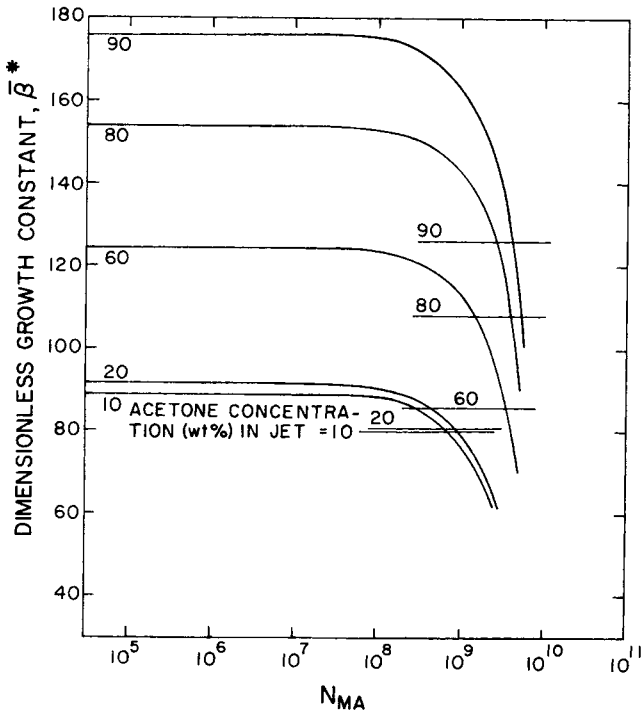

Fig. 10. Comparison of experimental and predicted growth constants for water jet breakup in the presence of acetone transferring out of the jet.

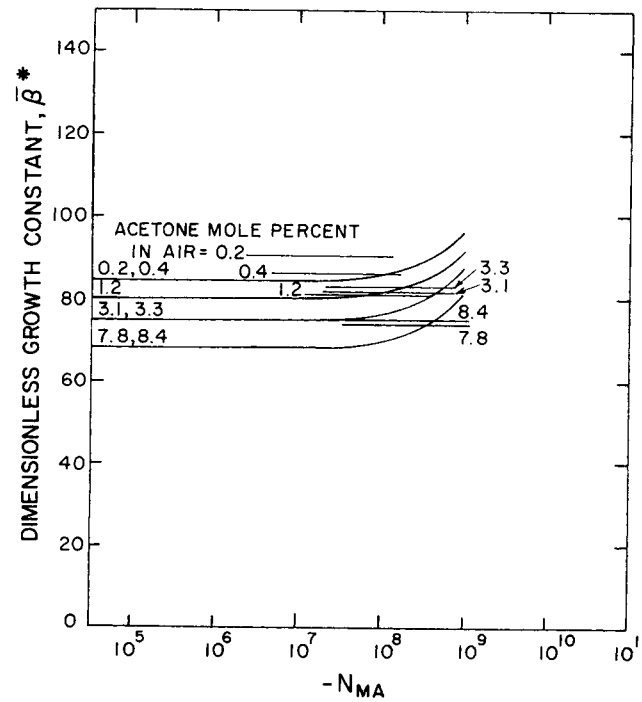

Fig. 11. Comparison of experimental and predicted growth constants for water jet breakup in the presence of acetone transferring into the jet.

ACKNOWLEDGMENTS

This research was supported by grants from the Office of Saline Water (U.S. Department of the Interior) and the National Science Foundation.

NOTATION

a = jet radius, cm
c = solute concentration disturbance, g-mole/cm^3
c^* = solute concentration in equilibrium with surroundings, g-mole/cm^3
$\mathcal{D}$ = solute diffusivity, cm^2/s
G_1-G_8 defined in Equation (13)
h = number of axes of symmetry about which the disturbance oscillates, dimensionless
i = $(-1)^{1/2}$
$I_h(\ )$ = modified Bessel function of the first kind, order h
k = disturbance wave number, cm^{-1}
K_c = proportionality constant, s^{-1}
$K_h(\ )$ = modified Bessel function of the second kind, order h
k_0 = mass transfer coefficient in the surroundings, cm/s
K_0 = k_0 times the solute distribution coefficient
L = jet length, cm
N_i = dimensionless groups defined in Table 1
p = pressure, dyne/cm^2
r = radial coordinate
R = gas constant
t = time, s
T = temperature, °K
u = velocity, cm/s
U = jet velocity, cm/s
z = axial coordinate

Greek Letters

β = growth constant, s^{-1}
$\overline{\beta}$ = dimensionless growth constant, $\beta\rho\, a^2/\mu$
Γ = solute adsorption, moles/cm^2
δ = adsorption equilibrium constant, cm
δ_m = mass transfer boundary layer thickness, cm
η = disturbance amplitude, cm
η_0 = initial disturbance amplitude, cm
θ = azimuthal coordinate
λ = disturbance wave length, cm
μ = viscosity, g/cm s
ν = kinematic viscosity, cm^2/s
ξ = dimensionless wave number
ξ_1, ξ_2 defined in Equation (13)
ρ = density, g/cm^3
σ = surface tension, g/s^2

Subscripts

a, s = at jet surface
i = initial
0 = undisturbed
r, z, θ = coordinates
∞ = surroundings
$*$ = most unstable

LITERATURE CITED

Alterman, Z., "Capillary Instability of a Liquid Jet," *Phys. Fluids*, **4**, 955 (1961).

Anshus, B. E., "The Effect of Surfactants on the Breakup of Cylinders and Jets," *J. Colloid Interface Sci.*, **43**, 113 (1973).

Berg, J. C., and A. Acrivos, "The Effect of Surface Active Agents on Convection Cells Induced by Surface Tension," *Chem. Eng. Sci.*, **20**, 737 (1965).

Burkholder, H. C., "The Effects of Surface Adsorption, Heat Transfer and Mass Transfer on the Stability of Capillary Jets," Ph.D. dissertation, Univ. Washington, Seattle (1973).

———., and J. C. Berg, "The Effect of Mass Transfer on Laminar Jet Breakup, II. Liquid Jets in Liquids," *AIChE J.*, **20**, 000 (1974).

Haenlein, A., *Forschung*, **2**, 139 (1932).

Handbook of Chemistry and Physics, CRC Publ. Co., Cleveland, Ohio (1962).

Kayser, W. V., and J. C. Berg, "Spontaneous Convection in the Vicinity of Liquid Meniscuses," *Ind. Eng. Chem. Fundamentals*, **10**, 526 (1971).

Levich, V. G., *Physicochemical Hydrodynamics*, Prentice Hall, Englewood Cliffs, N. J. (1962).

Linde, H., S. Pfaff, and Chr. Zirkel, "Strömungsuntersuchungen zur hydrodynamischen Instabilität flüssig-gasförmiger Phasengrenzen mit Hilfe der Kapillarspaltmethode," *Z. Phys. Chem.*, **225**, 72 (1964).

Ling, C.-H., and W. C. Reynolds, "Non-parallel flow corrections for the stability of shear flows," *J. Fluid Mech.*, **59**, 571 (1973).

Palmer, H. J., and J. C. Berg, "Hydrodynamic stability of surfactant solutions heated from below," *ibid.*, **51**, 385 (1972).

Pearson, J. R. A., "On convection cells induced by surface tension," *ibid.*, **4**, 489 (1958).

Plateau, M. T., *Statique Expérimentale et Théorique des Liquides soumis aux seules Forces Moléculaires*, Paris (1873).

Prandtl, L., *Fluid Dynamics*, Hafner, New York (1952).

Rayleigh, Lord, "On the Instability of Jets," *Proc. London Math. Soc.*, **10**, 4 (1878).

———., "On Capillary Phenomena of Jets," *Proc. Royal Soc. (London)*, **29**, 71 (1879).

———., "On the Instability of a Cylinder of Viscous Liquid under Capillary Force," *Phil. Mag.*, **34**, 145 (1892).

Savart, F., "Mémoire sur la Constitution des Veines Liquides Lancées par des Orifices Circulaires en mince paroi," *Ann. Chim. Phys.*, **53**, 337 (1833).

Sawistowski, H., "Interfacial Phenomena," in *Recent Advances in Liquid-Liquid Extraction*, C. Hanson, (ed.) Pergamon Press, Oxford (1971).

Sternling, C. V., and L. E. Scriven, "Interfacial Turbulence: Hydrodynamic Instability and the Marangoni Effect," *AIChE J.*, **5**, 514 (1959).

Sterling, A. M., "The Instability of Capillary Jets," Ph.D. dissertation, Univ. Washington, Seattle (1969).

Weber, C., "On the Breakup of a Fluid Jet," *Z. Angew. Math. Mech.*, **11**, 136 (1931).

Part II. Liquid Jets in Liquids

The instability and breakup of laminar liquid jets in liquid surroundings is investigated for situations where solute transfer across the jet interface renders the system susceptible to Marangoni convection. This work parallels Part I (Burkholder and Berg, 1974) on the effect of mass transfer on the breakup of laminar liquid jets in gases. Behavior in liquid-liquid systems, however, differs significantly from that for liquid-gas systems and cannot be inferred from the analysis of the latter. Linear hydrodynamic